Thermoresponsive Conductivity of Acrylamide-Based Polymers and Ni Microparticle Composites

Hayato Onishi, Yuta Koda, Hideo Horibe

Thermoresponsive Conductivity of Acrylamide-Based Polymers and Ni Microparticle Composites

Hayato Onishi,[1] Yuta Koda,*[1] and Hideo Horibe*[1]
[1]*Department of Applied Chemistry and Bioengineering, Graduate School of Engineering, Osaka City University, 3-3-138, Sugimoto, Sumiyoshi-ku, Osaka 558-8585, Japan*

E-mail: koda@ims.tsukuba.ac.jp; hhoribe@a-chem.osaka-cu.ac.jp

Composite materials with polymers and inorganic fillers enable the preparation of a variety of functional polymer materials. In particular, composites with the crystalline polymers and Ni microparticles (NiMPs) can be applied to the thermoresponsive conductive materials which are called as PTC (positive temperature coeffcient) materials. These materials are conductive around room temperature, and turn to insulators at high temperature. This phenomenon is induced by the volume expansion of the crystalline domains, therefore, the design of matrix polymers has been limited. Herein, we showed PTC phenomena by using polyacrylamide-based (co)polymers in lieu of crystalline polymers. Those materials showed PTC phenomena regarding conductivity probably owing to the hydrogen bonding, yet polyacrylamides are amorphous polymers.

Keywords: Thermoresponsibility, Polyacrylamides, Polymer Composite Materials

Organic–inorganic composite materials enable the preparation of a variety of functional materials.[1–5] In particular, polymer-based composite materials have been rapidly developed in both academic and industrial fields because polymer-based composites can be easily prepared just by melt-mixing. For example, crystalline polymer-based composites including Ni microparticles (NiMPs) exhibit thermoresponsive conductive function which is named as PTC phenomena regarding resistivity.[6–8] The materials are conductive around room temperature, and turn to insulators at high temperature. The temperature when the resistivity is 10 times as large as that at room temperature is defined as T_{PTC}. Such thermoresponsive function is resulted from not the glass transition (T_g) but the volume expansion of the crystalline polymers such as HDPE (high density polyethylene) around the melting points (T_m's). This is because the aggregation forms of NiMPs would be change at that time (Scheme 1b).[7] Owing to the mechanism, it is difficult to tune the temperature at which the conductivity changes. To resolve the problem, the aggregation of NiMPs in matrix will be changed by other factors except for the volume expansion around T_m.

Hydrogen bonds are dynamic bonds because the bond formation is affected by temperature.[9–12] For example, the solubility of poly(*N*-isopropylacrylamide) (poly(NIPAM)) and poly(2-oxazoline) in water depends on temperature because the hydrogen bonding between the polymer and water reversibly forms and deforms.[13–15] Around body temperature, those polymers exhibit lower critical solubility temperature (LCST)-type miscibility in water. The aggregation of those polymer chains can be tuned by hydrogen bonding. Therefore, intra- and intermolecular hydrogen bonding formation in bulk state of amide-based

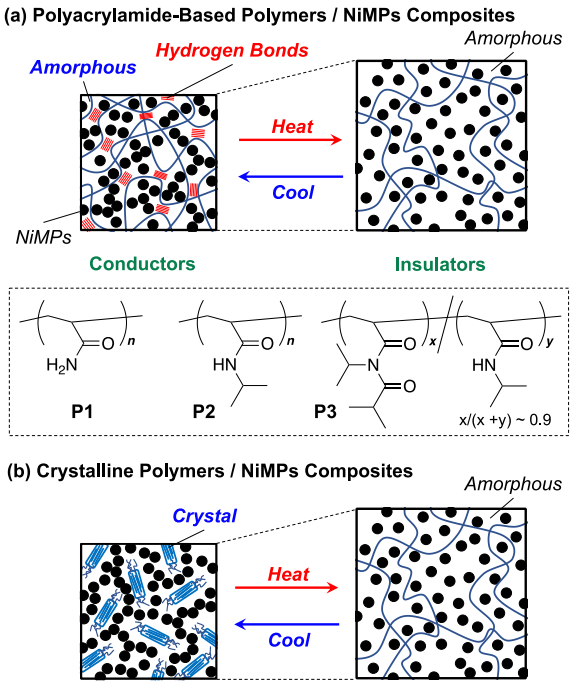

Scheme 1. Proposed Mechanisms of PTC Phenomenon in (a) Polyacrylamide-Based and (b) Crystalline Polymers / NiMPs Composite Materials[7]

polymers could be useful for the thermoresponsive function regarding the conductivity of polymer/NiMPs composites because the conductive path would be affective by the molecular chain dynamics.

Given the aforementioned background, polyacrylamide-based polymers and NiMPs composite materials were prepared to diversify the material design of the thermoswitchable conductive function (Scheme 1a). To achieve this, the primary or secondary polyacrylamides, and the copolymer of secondary and tertiary acrylamides were synthesized through single electron transfer living radical polymerization (SET-LRP) by using Haddleton's Cu-based catalytic system and polymer reaction.[16–19] The composite materials were prepared with the polyacrylamide-based (co)polymers by melt-mixing. The secondary polyacrylamide-based composite efficiently exhibited PTC phenomenon regarding resistivity probably owing to the

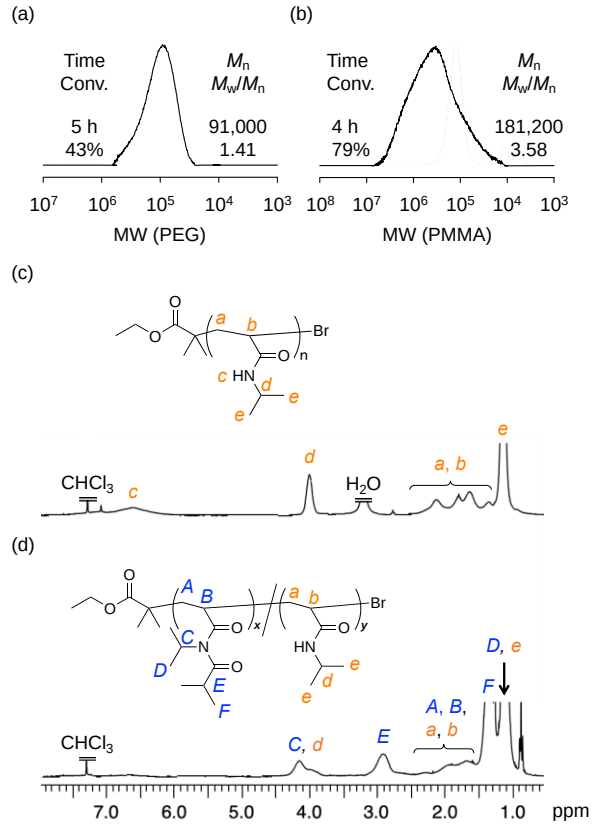

Figure 1. SEC curves of (a) **P1** and (b) **P2,** and ^{1}H NMR spectra (300 MHz, r.t.) in $CDCl_3$ of (c) **P2** and (d) **P3** ([polymer] = 30 mg/mL).[21]

intra- and intermolecular hydrogen bonds. This strategy in amorphous polymer-based composite will contribute to the further development of thermoswitchable conductive function of polymer-based composite materials and diversify the material design.

In our strategy, we tried to utilize the change of the molecular chain dynamics by cleaving hydrogen bonds in lieu of the volume expansion in the case of crystalline polymer-based composite materials. Therefore, the molecular weight of acrylamide-based polymers were roughly controlled by LRP to reduce the effect of amorphous chain dynamics such as chain entanglements.[20] Acrylamide was polymerized in water through SET-LRP by using a pair of CuBr and Me_6-TREN (tris[2-(dimethylamino)ethyl]amine) at 0 °C (Scheme S2).[18,19] For the control of the polymerization of acrylamide, a water-soluble bromide initiator bearing a hydroxy group was used because a hydrophilic initiator is preferred for the polymerization of acrylamide in pure water by SET-LRP. Acrylamide was smoothly consumed up to ~ 43% in 5 h, and polyacrylamide (**P1**) was obtained (Figure 1; M_n(SEC) = 91,000, M_w/M_n = 1.41). Owing to the difficulty of the polymerization of acrylamide by LRP, its molecular weight distribution (MWD) was relatively wide. After the

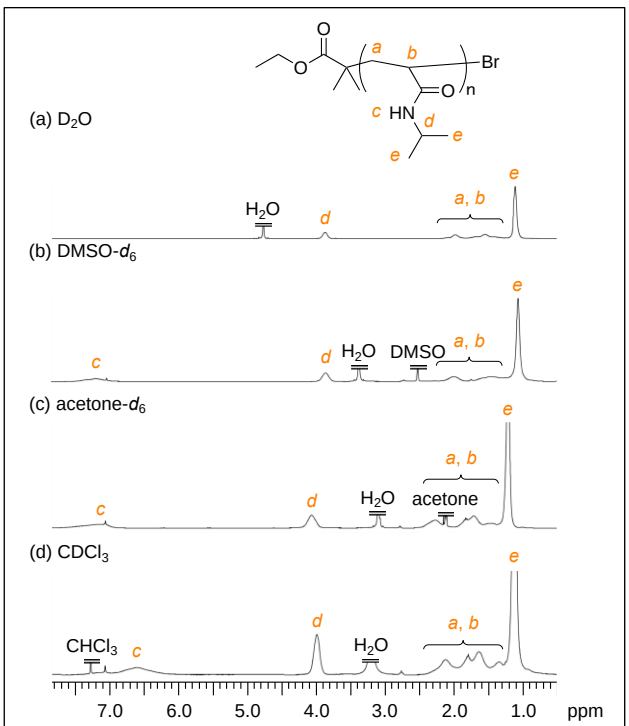

Figure 2. ^{1}H NMR spectra (300 MHz, r.t.) of **P2** in (a) D_2O, (b) DMSO-d_6, (c) acetone-d_6, and (d) $CDCl_3$ ([polymer] = 30 mg/mL).

purification of **P1**, the successful synthesis of **P1** was confirmed by ^{1}H NMR (Figure S3).

To synthesize secondary polyacrylamdies, NIPAM was polymerized in water / CH_3CN (= 95/5, v/v) through SET-LRP by using the same pair of CuBr and Me_6-TREM at 0 °C (Scheme S3).[16,17,19] NIPAM was smoothly consumed up to ~ 79% in 5 h, poly(NIPAM) was obtained (**P2**; Figure 1; M_n(SEC) = 181,000, M_w/M_n = 3.58). To weaken hydrogen bonding in **P2**, the amide proton in **P2** (peak ***c*** in Figure 1c) was capped by isobutyl chloride, and acrylamide-based copolymer (**P3**) was synthesized. To prepare **P3**, **P2** was reacted with much excessive isobutyl chloride in chloroform after the purification (Scheme S4). Analyzed by ^{1}H NMR, **P2** and **P3** clearly showed all proton signals assignable to **P2** and **P3**.[21] Amide proton (peak ***c*** in **P2**) mostly disappeared, and the much broaden peak ***E*** also appeared in the spectrum of **P3**. Furthermore, peak areas of (***D*** + ***e***) and ***F*** were almost same (***D*** + ***e***: ***F*** = 1.14 : 1.0 ~ 1.1 : 1.0). The functionality was calculated by those peaks although the peaks were partially overlapped. This was because the peaks of side chains (***e***, ***D***, and ***F***) were sharper than other peaks from the main chains (***a***, ***b***, ***d***, and **A**–**C**). The functionality was roughly determined as ~ 0.9 because those peaks were partially overlapped. Thus, hydrogen bonding in **P3** would be much weaker than that in **P2**.

To evaluate hydrogen bonding of **P2**, **P2** was characterized by ^{1}H NMR in several solvents (Figure 2; D_2O, DMSO-d_6, acetone-d_6, $CDCl_3$). In D_2O, peak ***c*** from the amide proton was not observed owing to proton exchange. However, peak ***c*** shifted to the lower magnetic fields

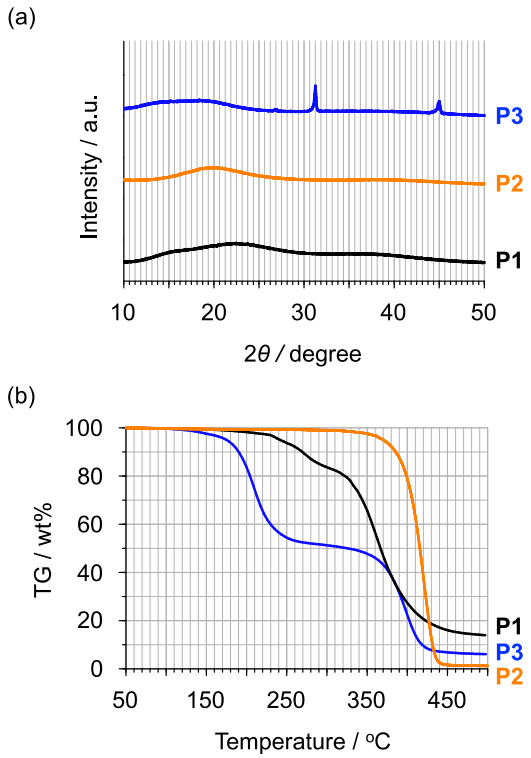

Figure 3. (a) XRD patterns and (b) TG curves of (black) **P1**, (orange) **P2**, and (blue) **P3** (heating rate = 10 °C/min).

depending on the increment of Dimroth and Reichardt's transition energy ($E_T(30)$) because of the solvation around amide groups by hydrogen bonds (DMSO-d_6 > acetone-d_6 > $CDCl_3$; $E_T(30)$ = 62.0 (H_2O), 44.8 (DMSO), acetone (41.6), 39.5 (chloroform)).[22,23] Furthermore, the peaks from acrylamide-backbone disappeared, suggesting that the main chains aggregated in DMSO-d_6 and D_2O. On the other hand, the hydrogen bonding formation in the pellet state of **P2** was observed in FT-IR spectrum (Figure S4).

To characterize bulk properties, **P1** – **P3** were analyzed by X-ray diffraction (XRD) and thermogravimeter (TG) (Figure 3). In general, polyacrylate and polyacrylamide are amorphous. Indeed, XRD patterns of **P1** – **P3** showed broad peaks, indicated that those polymers formed disordered states in their bulk (Figure 3a). Small peaks would resulted from a little amount of the salt generated in polymer reaction. Before the preparation of composite materials, thermostability was investigated to decide melt-blending condition of polymers and NiMPs (Figure 3b). Under N_2 gas flow, all polymers were heated from 50 to 500 °C (heating rate = 10 °C/min). The weight of **P1** gradually decreased around 230 °C, and dramatically decreased around 300 °C. That of **P2** decreased from ~ 350 °C by one step. On the other hand, the weight of **P3** first decreased from 150 °C and secondarily decreased from 350 °C. Compared with **P2**, the first decrease in **P3** resulted from the change from the tertiary to secondary polyacrylamide, and the second decrease derived from the decomposition of polymer chains. In the first step, furthermore, TG decreased to approximately 50%. This

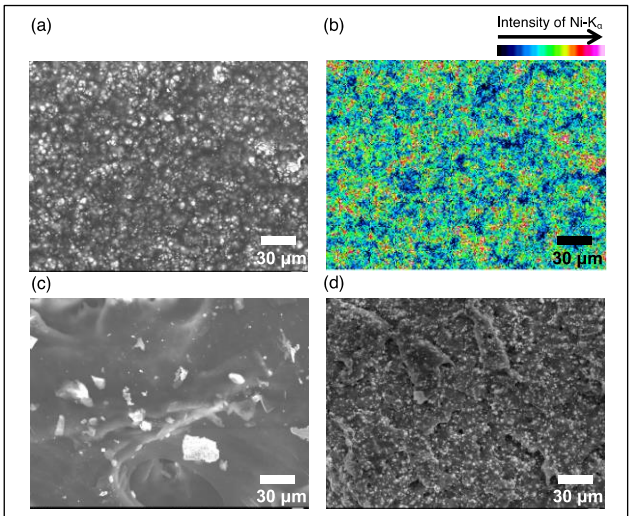

Figure 4. (a, c, d) SEM images and (b) elemental mapping of NiMPs in (a, b) **P2**, (c) **P3**, and (d) HDPE / NiMPs composite materials (φ_{Ni} = 20vol%).

result also supported that the copolymers were mostly composed of the tertiary acrylamide units by polymer reaction. As a consequence, **P1** and **P2** were melt-mixed with NiMPs at 200 °C, and **P3** was done at 110 °C in the next step.

P1, **P2**, and **P3** were melt-mixed with NiMPs at 200 or 110 °C for 15 min (mixing rate = 60 rpm) for the preparation of the composite materials. In this process, the NiMPs composite with **P1** was not prepared at all because **P1** was the less processability probably owing to the stronger hydrogen bonding. Eventually, the composite materials with **P2** and **P3** were prepared by melt-mixing. Prepared composite materials were characterized by SEM (scanning electron microscope) coupled with or without EDS (energy dispersive X-ray spectroscopy) (Figure 4, Figure S5). The SEM image of **P2**/NiMPs showed that NiMPs were almost homogeneously blended in **P2**, yet the SEM image of **P3**/NiMPs indicated that NiMPs did not dispersed well in **P3** probably owing to the melt-mixing at the lower temperature. The EDS mapping of **P2**/NiMPs also exhibited that NiMPs were distributed in **P2** as well as those of the previous composite materials of NiMPs with HDPE and PMMA (poly(methyl methacrylate)) (Figures 4d and S5).

Thermoresponsive conductivity of **P2**, **P3**, HDPE, and PMMA composites with NiMPs were characterized by 2-terminal method, and those materials were heated from 30 to 110 °C (Figure 5). In the case of **P3**/NiMPs, the conductivity around room temperature was the relatively higher than those of other composites, and the increment of conductivity stopped. Then, **P3**/NiMPs showed NTC (negative temperature coefficient) phenomenon regarding resistivity, and the resistivity gradually decreased. These results were probably because NiMPs did not disperse in the matrix well. On the other hand, **P2**/NiMPs showed the lower conductivity around room temperature, and exhibited PTC phenomenon on conductivity (T_{PTC} = 81 °C) such as HDPE/NiMPs, yet **P2** is the amorphous polymer. Compared with **P3**, **P2** was more

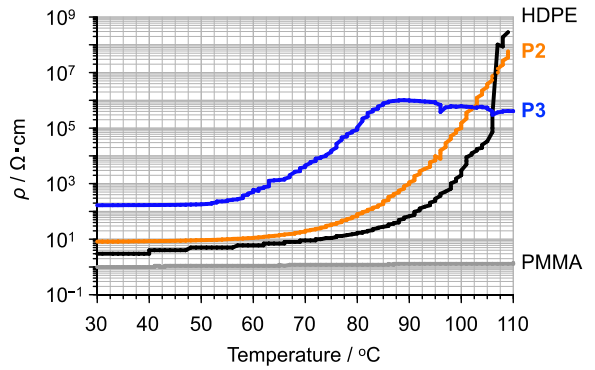

Figure 5. Resistivity-temperature curves of (orange) **P2**, (blue) **P3**, (black) HDPE, and (gray) PMMA / NiMPs composite materials (φ_{Ni} = 20vol%).

suitable matrix for PTC materials because the resistivity at room temperature of **P2**/NiMPs was much lower than that of **P3**/NiMPs composites. It was also because NTC phenomenon on resistivity did not occur in **P2**/NiMPs by heating. On the other hand, PMMA/NiMPs did not show PTC phenomenon at all because PMMA has no crystalline phase in the bulk. This result also indicated that PTC did not occur at T_g (~ 100 °C). This would be because glass transition is not phase transition but just the starting point at which Brownian motion is released. Thus, the dispersity of NiMPs would be hardly change just by glass transition. Furthermore, the continuous increase of the resistivity cannot be explained only by T_g. Together, those results indicated the promise that intra- and intermolecular hydrogen bonding in **P2** would be effective to induce PTC phenomenon such as HDPE/NiMPs. Therefore, polymer design is very important for the preparation of PTC materials. This work shows the promise that the amorphous polymers having hydrogen bonding are possible to be applied to PTC materials, contributing to the further development of the thermoresponsive conductive materials.

In conclusion, polyacrylamide-based composite materials with NiMPs were prepared for the new type of thermoresponsive conductive materials. Polyacrylamide, polyNIPAM and its copolymer were prepared through SET-LRP with the pair of CuBr and Me_6-TREN in water and polymer reaction in chloroform. **P2** and **P3** were suitable as the matrix for the preparation of NiMPs composite materials. Then, only **P2**/NiMPs showed the low resistivity at room temperature and PTC phenomenon regarding conductivity such as HDPE/NiMPs, yet **P2** was the amorphous polymer. This result indicated the promise that intra- and intermolecular hydrogen bonds would induce the PTC phenomenon. **P2** was more suitable matrix for PTC materials than **P3**. This result proposed that amorphous polymers are possible to be applied to PTC materials by designing polymer structures. In addition, amorphous polymer-based composites have the potential that they will not show hysteresis, although crystalline polymer-based composites often show hysteresis owing to the gap between the T_m and the crystallization temperature (T_c). Therefore, polyacrylamide-based polymers will diversify the material designs of PTC materials to develop the thermoresponsive devises in the near future.

Supporting Information is available on http://dx.doi.org/10.1246/cl.******.

References and Notes

1 J. L. Abot, G. Bardin, C. Sprigel, Y. Song, V. Raghavan, N. Govindaraju, *J. Compos. Mater.* **2010**, *45*, 321–340.
2 S. A. Ju, K. Kim, J. H. Kim, S. S. Lee, *ACS Appl. Mater. Interfaces* **2011**, *3*, 2904–2911.
3 A. M. Beese, S. Sarkar, A. Nair, M. Naraghi, Z. An, A. Moravsky, R. O. Loutfy, M. J. Buehler, S. T. Nguyen, H. D. Espinosa, *ACS Nano* **2013**, *4*, 3434–3446.
4 L. Amirova, A. Surnova, D. Balkaev, D. Musin, D. Amirov, A. M. Dimiev, *ACS Appl. Mater. Interfaces* **2017**, *13*, 11909–11917.
5 M. Ochi, R. Takahashi, A. Terauchi, *Polymer* **2001**, *42*, 5151–5158.
6 A. Kono, K. Shimizu, H. Nakano, Y. Goto, Y. Kobayashi, T. Ougizawa, H. Horibe, *Polymer* **2012**, *53*, 1760–1764.
7 A. A. Snarskii, D. Zorinets, M. Shamonin, V. M. Kalita, *Physica A* **2019**, *535*, 122467.
8 B. Pourabbas, S. J. Peighambardoust, *J. Appl. Polym. Sci.* **2007**, *105*, 1031–1041.
9 Y. Koda, D. Takahashi, S. Sasaki, K. Akiyoshi, *ACS Appl. Bio Mater.* **2019**, *2*, 1920–1930.
10 Y. Koda, T. Terashima, M. Sawamoto, *ACS Macro Lett.* **2015**, *4*, 1366–1369.
11 Y. Koda, T. Terashima, M. Sawamoto, *Macromolecules* **2016**, *49*, 4535–4543.
12 V. Aseyev, H. Tenhu, F. Winnik, *Adv. Polym. Sci.* **2011**, *242*, 29–89.
13 Y. J. Zhang, S. Furyk, D. E. Bergbreiter, P. S. Cremer, *J. Am. Chem. Soc.* **2005**, *127*, 14505–14510.
14 D. Roy, W. L. A. Brooks, B. S. Sumerlin, *Chem. Soc. Rev.* **2013**, *42*, 7214–7243.
15 C. Weber, R. Hoogenboom, U. S. Schubert, *Prog. Polym. Sci.* **2012**, *37*, 686–714.
16 Q. Zhang, P. Wilson, Z. Li, R. McHale, J. Godfrey, A. Anastasaki, C. Waldron, D. M. Haddleton, *J. Am. Chem. Soc.* **2013**, *135*, 7355–7363.
17 F. Alsubaie, A. Anastasaki, V. Nikolaou, A. Simula, G. Nurumbetov, P. Wilson, K. Kempe, D. M. Haddleton, *Macromolecules* **2015**, *48*, 6421–6432.
18 G. R. Jones, Z. Li, A. Anastasaki, D. J. Lloyd, P. Wilson, Q. Zhang, D. M. Haddleton, *Macromolecules* **2016**, *49*, 483–489.
19 A. Anastasaki, V. Nikolaou, G. Nurumbetov, P. Wilson, K. Kempe, J. F. Quinn, T. P. Davis, M. R. Whittaker, D. M. Haddleton, *Chem. Rev.* **2016**, *116*, 835–877.
20 H. Watanebe, *Polym. J.* **2009**, *41*, 929–950.
21 Y. Kimura, T. Terashima, M. Sawamoto, *Macromol. Chem. Phys.* **2017**, *218*, 1700230.
22 Y. Marcus, *J. Solution Chem.* **1991**, *20(9)*, 929–944.
23 Y. He, J.-C. Eloi, R. L. Harniman, R. M. Richardson, G. R. Whittell, R. T. Mathers, A. P. Dove, R. K. O'Reilly, I. Manners, *J. Am. Chem. Soc.* **2019**, *141*, 19088–19098.
24 Present Address of Y. K.: Department of Materials Science, Faculty of Pure and Applied Sciences, University of Tsukuba, Tennoudai 1-1-1, Tsukuba, Ibaraki 305-8573, Japan

Graphical Abstract

Textual Information

A brief abstract	Theremoresponsive conductive materials were produced by polyacrylamide-based polymers and Ni microparticles. The materials exhibited PTC (positive temperature coeffcient) phenomenon regarding electric resistivity, yet such PTC phenomena had been observed only in crystalline polymer-based composite materials. Our strategy by using polyacrylamides will contribute to the development of PTC materials by diversifying the material design.
Title	Thermoresponsive Conductivity of Acrylamide-Based Polymers and Ni Microparticle Composites
Authors' Names	Hayato Onishi, Yuta Koda, Hideo Horibe

Graphical Information

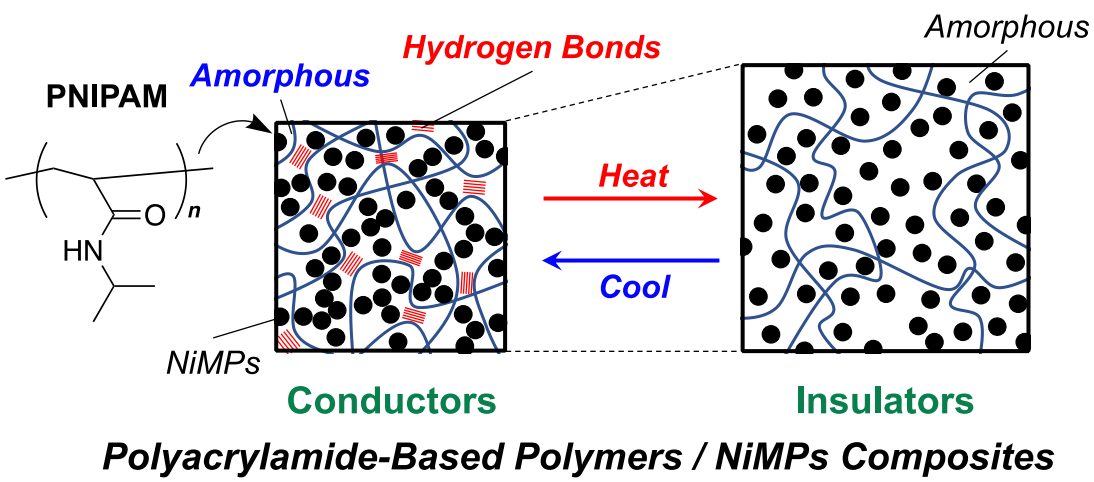

Polyacrylamide-Based Polymers / NiMPs Composites